

1 **This article was accepted for publication on 1st July 2019 and can be**
2 **downloaded here <https://doi.org/10.1016/j.pep.2019.105447>**

3 **Title:** Expression, purification and metal utilization of recombinant SodA from
4 *Borrelia burgdorferi*

5 **Author names and affiliations.**

6 Brown, G^a., Broxham, A.H^a., Cherrington, S.E^a., Thomas, D.C^a., Dyer, A^{a1}.
7 Stejskal, L^{a2}. & Bingham, R.J^a.

8
9 ^aDepartment of Biological and Geographical Sciences, School of Applied
10 Sciences, University of Huddersfield, Queensgate, Huddersfield, UK, HD1
11 3DH.

12 ¹Present Address: School of Immunology & Microbial Sciences, Faculty of Life
13 Sciences & Medicine, King's College London, Guy's Hospital, London, SE1
14 9RT.

15 ²Present Address: Institute of Structural and Molecular Biology, Birkbeck
16 College, London, UK

17 Corresponding author Richard J. Bingham, Email Address:

18 r.j.bingham@hud.ac.uk.

19

20 **Abstract**

21 *Borrelia* are microaerophilic spirochetes capable of causing multisystemic
22 diseases such as Lyme disease and Relapsing Fever. The ubiquitous Fe/Mn-
23 dependent superoxide dismutase (SOD) provides essential protection from
24 oxidative damage by the superoxide anion. *Borrelia* possess a single SOD
25 enzyme - SodA that is essential for virulence, providing protection against
26 host-derived reactive oxygen species (ROS). Here we present a method for
27 recombinant expression and purification of *Borrelia burgdorferi* SodA in *E. coli*.
28 Metal exchange or insertion into the Fe/Mn-SOD is inhibited in the folded
29 state. We therefore present a method whereby the recombinant *Borrelia* SodA
30 binds to Mn under denaturing conditions and is subsequently refolded by a
31 reduction in denaturant. SodA purified by metal affinity chromatography and
32 size exclusion chromatography reveals a single band on SDS-PAGE. Protein
33 folding is confirmed by circular dichroism. A coupled enzyme assay
34 demonstrates SOD activity in the presence of Mn, but not Fe. The apparent
35 molecular weight determined by size exclusion corresponds to a dimer of
36 SodA; a homology model of dimeric SodA is presented revealing a surface
37 Cys distal to the dimer interface. The method presented of acquiring a target
38 metal under denaturing conditions may be applicable to the refolding of other
39 metal-binding proteins.

40

41

42

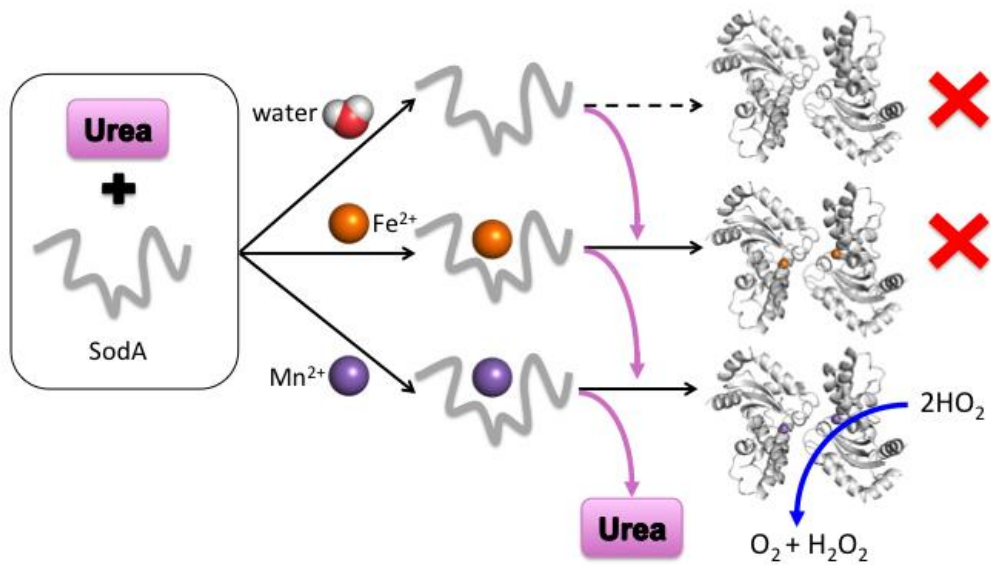
43

44 **Keywords:** *Borrelia*; Superoxide dismutase; Manganese; *E. coli*

45

46

47 **Graphical abstract**
48



49
50
51
52
53
54
55
56
57
58

Highlights

- Recombinant *Borrelia burgdorferi* SodA is active in the presence of Mn, but not Fe
- *B. burgdorferi* SodA is a homodimer
- Recombinant *B. burgdorferi* SodA can be refolded from 8M urea in the presence of Mn

59 **Acknowledgements**

60 Circular dichroism was collected at the University of York with the kind
61 assistance of Dr. Andrew Leech.

62 1. Introduction

63 Superoxide ($O_2^{\bullet-}$), formed by the reduction of O_2 , is a reactive free radical
64 capable of generating numerous other free radicals and reactive oxygen
65 species that may go on to damage cellular components [1]. Superoxide
66 dismutase (SOD) is highly conserved throughout all domains of life and
67 catalyzes the dismutation of $O_2^{\bullet-}$ to hydrogen peroxide (H_2O_2) [2]. The most
68 ancient form, thought to have evolved over 2 Gyr ago, is the Fe/Mn-SOD [3].
69 Found in mitochondria (SOD2) and the cytoplasm of bacteria, the Fe/Mn-SOD
70 exists as either a homodimer or homotetramer with one metal-binding site per
71 chain [2].

72
73 *Borrelia burgdorferi* is a pathogenic spirochete with several characteristics
74 that are dissimilar to other prokaryotes, including an unusual genome
75 structure [4], extremely limited metabolic capacity [5], and the presence of
76 polyunsaturated membrane lipids [6]. *Borrelia* is also highly unusual in its
77 ability to grow without needing a source of Fe [7], instead its cellular
78 metabolism has evolved to utilize Mn, which is imported to significant
79 concentrations by the specific transporter BmtA [8]. No iron-specific enzymes
80 have been identified in *Borrelia*, however Fe-binding proteins have been
81 identified that play a role in Cu/Fe detoxification [9]. The lack of cellular Fe
82 gives some protection against oxidative damage to DNA by Fenton chemistry.
83 The major targets of host-derived reactive oxygen species are the
84 polyunsaturated membrane lipids [6].

85 While a small number of SOD-enzymes have been identified that remain
86 catalytically active with either Mn or Fe bound at the active site (cambialistic
87 SODs), the majority have evolved to function only in the presence of their
88 target metal ion and are named correspondingly as either Fe-SOD or Mn-
89 SOD. Fe/Mn-SODs bind to either metal with the same trigonal-bipyramidal
90 geometry, and have high sequence and structural homology [10]. Metal
91 coordinating residues (His26, His81, Asp167 and His171 based on *E. coli*
92 numbering) are identical between the Mn and Fe-SODs and mis-incorporation
93 can occur. Metal selectivity is thought to be at least partly driven by
94 bioavailability. Predicting metal specificity from protein sequence alone is
95 challenging [11].

96 The genome of *Borrelia burgdorferi* contains a single SOD (*sodA*, bb0153),
97 which was demonstrated to be essential for infectivity in a mouse model [12].
98 The inactivation of *sodA* resulted in a phenotype more vulnerable to challenge
99 by activated macrophages and neutrophils, while *in vitro* growth was
100 unaltered. Although early work suggested this might be an Fe-SOD [13], it
101 was subsequently demonstrated to utilize Mn [14]. An elegant series of *in vivo*
102 experiments demonstrated that *Borrelia* accumulates high levels of cellular
103 Mn, and that this is required to activate the SodA enzyme. In contrast, *Borrelia*
104 SodA expressed in the iron-rich environment of yeast mitochondria was
105 inactive [14].

106 Previous studies of the metal utilization of *Borrelia* SodA have not used pure
107 SodA, rather assays based on non-denaturing electrophoresis gels with
108 *Borrelia* whole cell lysate [13, 15] or purified cell extracts [14]. In addition, no

109 studies to date have conclusively determined whether this enzyme is
110 cambialistic, whereby it could use both manganese and iron as its co-factor.
111 Therefore, the objective of this work was to produce and purify recombinant
112 *Borrelia* SodA allowing *in vitro* investigation of enzyme activity in the presence
113 of Mn and Fe. Here we report a method to produce sufficient quantity of SodA
114 to allow structural and biochemical studies. We describe a protocol that
115 utilizes addition of Mn and Fe salts to recombinant protein in the denatured
116 state prior to refolding and purification, thereby preventing contamination of
117 downstream processes with these reactive transition metal ions. A homology
118 model of dimeric SodA is presented.

119 *2. Material and Methods*

120 *2.1 Plasmid construction and gene expression*

121 The *bb0153* gene was codon optimized for expression in *E. coli*, synthetically
122 produced (Eurofins Genomics) and sub-cloned into pET-47b(+) (Novagen®).
123 The resulting construct was transformed into T7 Express Competent *E. coli*
124 (New England BioLabs). Transformed cells were grown in LB media at 37 °C
125 in an orbital incubator and were induced at an OD₆₀₀ of 0.6 by addition of
126 isopropyl-β-D-1-thiogalactopyranoside (IPTG, Sigma-Aldrich) to a working
127 concentration of 1 mM. After 4-hours, induced cells were harvested by
128 centrifugation and lysed on ice by pulsed sonication in 0.3 M NaCl, 50 mM
129 Tris-HCl, pH 8.0.

130

131 *2.2 Purification of inclusion bodies*

132 The soluble fraction was removed by centrifugation (20,000 x g for 30 min at
133 4 °C), the insoluble material was resuspended in 0.3 M NaCl, 50 mM Tris-HCl,
134 pH 7 and briefly pulse sonicated at an amplitude of 40% for a total length of
135 30 seconds. DNase1 was added at 1 µg/ml and the solution incubated at 4 °C
136 for 4 hours. Following incubation, samples were centrifuged (20,000 x g for 30
137 min at 4 °C) and weighed prior to re-suspension in Wash Buffer 1 (Table 1) at
138 10 ml per gram of pellet. The suspension was briefly sonicated as previously
139 described. Following this, the suspension was subjected to low speed
140 centrifugation (~8000 x g) until a firm pellet was obtained. This process was
141 repeated twice with inclusion Wash Buffer 1, twice with Wash Buffer 2, and
142 twice with Wash Buffer 3 (Table 1). The inclusion bodies were then solubilized
143 in Denaturing Buffer overnight at room temperature with shaking.

144

Wash Buffer 1	0.3 M NaCl, 50 mM Tris-HCl, 1 mM EDTA, 10 mM DTT, 5 % Triton X-100, pH 8.0
Wash Buffer 2	0.3 M NaCl, 50 mM Tris-HCl, 1 % Triton X-100, pH 8.0
Wash Buffer 3	0.3 M NaCl, 50 mM Tris-HCl, pH 8.0
Denaturing Buffer	8 M urea, 0.3 M NaCl, 50 mM Tris-HCl, pH 8.0

145

146 Table 1. Buffers for inclusion-body wash procedure.

147

148 *2.3 Purification of metal-free protein*

149 Divalent metal ions present in the re-suspended bacterial pellet were removed
150 by utilizing unchelated nitrilotriacetic acid (NTA). A 5 ml Ni-NTA column (His-
151 Trap HP, GE Healthcare) was stripped of Ni²⁺ by addition of 100 mM EDTA.
152 After equilibration of the column with Denaturing Buffer (8 M urea, 0.3 M NaCl,
153 50 mM Tris-HCl, pH 8.0), the resuspended pellet (volume 20 ml) was passed
154 through the column twice to bind any free metal ions at a flow rate of 0.5
155 ml/min using an AKTA Prime FPLC system.

156

157 *2.4 Addition of metal co-factors*

158 Following the removal of metal ions by NTA the pH of the denatured protein
159 solution was decreased to pH 4.0 by slow addition of dilute HCl. Acidification
160 of the solution was required to both increase the solubility and minimize the

161 oxidation of Fe²⁺. MnCl₂ or FeCl₂ were added to samples of recombinant
162 SodA to a final concentration of 1 mM. Recombinant protein samples were
163 incubated at 4°C overnight before the pH was increased back to pH 8.0 by
164 slow addition of dilute NaOH.

165

166 *2.5 On-column refolding and purification*

167 Recombinant protein samples (with addition of either MnCl₂ and FeCl₂ or
168 control) were subjected to centrifugation at 16,000 g for 30 minutes prior to
169 refolding/purification using a His-Trap HP column (GE Healthcare). The
170 column was equilibrated with 10 column volumes (CV) of denaturing buffer (8
171 M urea, 50 mM Tris-HCl, 0.3 M NaCl, pH 8.0) and recombinant protein loaded
172 at 0.5 ml/min. Protein folding was achieved by washing with a linear gradient
173 from 8 M to 1 M urea over 2 hours in 50 mM Tris-HCl, 0.3 M NaCl, pH 8.0
174 (flow rate 0.5 ml/min). The column was then washed with 10 column volumes
175 of 1 M urea, 50 mM Tris-HCl, 0.3 M NaCl, 50 mM imidazole, pH 8.0.
176 Recombinant protein was eluted in 50 mM Tris-HCl, 0.3 M NaCl, 0.3 M
177 imidazole at pH 8.0.

178

179 Size Exclusion Chromatography was carried out using a Superdex 75 10/300
180 GL column (GE Healthcare) in 50 mM Tris-HCl, 0.3 M NaCl at pH 8.0. The
181 exclusion volume/void volume was determined using blue dextran (molecular
182 mass of ~2,000 kDa) which eluted at 8.7 ml. Apparent molecular weights
183 were determined by comparison with a calibration curve prepared using
184 known protein standards (Sigma-Aldrich).

185

186 Mn-SodA, Fe-SodA and apo-SodA were concentrated using a 10NMWL
187 Amicon Ultra-15 centrifugal filter unit (Merck Millipore), centrifuged at 16,000 x
188 g for 20 min at room temperature and protein concentrations ascertained by
189 UV spectroscopy (extinction coefficient 38390 M⁻¹cm⁻¹) and Bradford analysis
190 [16].

191 *2.6 Circular dichroism*

192 Circular dichroism experiments were carried out on a Jasco J-810
193 spectropolarimeter. Air and buffer blank background data were acquired and
194 experimental measurements taken over a wavelength range of 185- 260 nm.
195 Experimental data was obtained at a protein concentration of 0.1 mg/ml over
196 five individual scans and averaged. Data were analyzed using DichroWeb [17,
197 18] using a mean residue weight of 111.8 Da, corresponding to the mean
198 residue weight of SodA. Algorithms used for deconvolution included CDSSTR,
199 CONTIN and SELCON3 with the SP175 reference set.

200

201 *2.7 SOD enzyme activity assay*

202 Superoxide dismutase activity was measured by an indirect enzyme assay
203 (SOD Assay Kit, 19160, Sigma-Aldrich) and carried out according to the
204 manufacturer's instructions with additional negative controls to account for
205 possible interference from the utilized buffers. The assay was used to
206 compare activity rates of recombinant Mn-SOD, Fe-SOD and apo-SOD and
207 was run in quadruplicates with a protein concentration of 100 µg/ml in 96
208 well plates in a total well volume of 240 µl. Formazan dye production was
209 determined by measuring absorbance for 20 minutes at 440 nm using a BMG
210 Labtech SPECTROstar Nano microplate-reader. Statistical analysis by
211 ANOVA and a multiple comparison of sample means by Tukey's test
212 (TukeyHSD) was conducted in R [19].
213

214 *2.8 Homology modelling*

215 A homology model of *B. burgdorferi* SodA (UniProtKB accession code
216 O30563) was generated using Phyre2 using intensive mode [20]. The highest
217 ranked template was the Mn-dependent SOD from *Thermus thermophilus*
218 with 50% sequence identity over 201 residues. The homodimer was
219 generated by superimposition of the Phyre2 model onto the dimers of Mn-
220 SOD from *E. coli* and *T. thermophilus* (PDB accession codes 1D5N and
221 3MDS). Molecular graphics and analyses were performed with UCSF
222 Chimera, developed by the Resource for Biocomputing, Visualization, and
223 Informatics at the University of California, San Francisco [21].

224

225 **3. Results and discussion**

226 *3.1 Cloning, expression and initial purification of SodA inclusion bodies*

227 The coding sequence for gene bb0153 was synthesized and incorporated into
228 the MCS of pET-47b(+) for expression of *B. burgdorferi* SodA with an N-
229 terminal 6xHis-tag. Induction of T7 Express cells with IPTG resulted in high
230 levels of SodA expression in inclusion bodies (Fig. 1A). No detectable
231 recombinant protein was found in the soluble fraction despite attempts to
232 optimize expression conditions such as: induction temperature, IPTG
233 concentration and the addition of ethanol [22] (results not shown). A series of
234 pellet-wash steps were employed (Methods section 2.2) to isolate inclusion
235 bodies and remove background contamination (Fig. 1B).

236 *3.2 Metal insertion*

237 A range of factors contributed to our experimental approach to metal insertion
238 under denaturing conditions. Buffers containing free transition metal ions may
239 effectively catalyze the dismutation of oxygen radicals in the absence of
240 enzyme. In addition, because of the neutral pH and oxidizing conditions, the
241 addition of even small concentrations of Fe²⁺ metal salts resulted in insoluble
242 oxidation products that may interfere with subsequent colorimetric SOD
243 assays. Furthermore, *in vitro* studies using *E. coli* Mn-SOD showed that the
244 direct reconstitution of metal ions by dialysis is not always possible [23]. *In*
245 *vivo* studies have demonstrated that the folded form of apo-SOD2 (the
246 mitochondrial homologue of *Borrelia* SodA with 40% sequence identity) could
247 not acquire Mn and that protein unfolding was required during mitochondrial
248 import for metal binding and activation [24]. For these reasons, it was decided
249 that Fe and Mn ions would be added to *Borrelia* SodA prior to refolding. The
250 subsequent purification steps employed (Ni-NTA and size exclusion
251 chromatography) also served to remove unbound metal ions and prevent
252 interference with subsequent colorimetric SOD assays.

253 To generate denatured apo-SodA, inclusion bodies were washed in EDTA
254 buffer, solubilized in 8M urea, and any residual metal ions were removed by
255 passing the solution through stripped NTA resin. Metal salts (or water control)
256 were then added to protein solutions in denaturing conditions to generate
257 samples of apo-SodA, Fe-SodA and Mn-SodA. Centrifugation was required to
258 remove insoluble oxidation products. All three samples (apo-SodA, Fe-SodA
259 and Mn-SodA) were then refolded and purified independently.

260 *3.3 Protein folding and final purification*

261 Denatured protein samples were bound to Ni-NTA resin and allowed to refold
262 by a slow reduction in urea concentration over 2 hours. Protein was eluted by
263 the addition of imidazole resulting a single band on SDS-PAGE (Fig. 1C). Size
264 exclusion chromatography was utilized to remove misfolded or aggregated
265 protein (Fig. 1D). Three peaks were detected, the first of which corresponded
266 with the void volume (>2000 kDa) and is most likely mis-folded/aggregated
267 protein. The elution volumes of the two subsequent peaks correspond almost
268 exactly to dimeric (43 kDa) and monomeric (23.5 kDa) SodA, and both peaks

269 were confirmed to contain SOD activity by enzyme assay. The minor peak
 270 corresponding to monomeric SodA is most likely an artifact of recombinant
 271 expression and is unlikely to be physiologically relevant. Bacterial MnSod
 272 enzymes are most frequently dimeric [25], therefore the major peak detected
 273 from size exclusion that corresponds to dimeric SodA was selected for further
 274 study. The yield of refolded proteins were similar for Mn and Fe-SodA (8 mg
 275 purified protein per liter of *E. coli* cell culture). The yield of apo-SodA was
 276 particularly low at 0.9 mg/l.

277

278 Protein folding was confirmed by circular dichroism (CD) spectroscopy (Fig. 2,
 279 Table 2). Apo-SodA, Fe-SodA and Mn-SodA were confirmed to have CD
 280 spectra with high helix content (~60%) consistent with the long alpha-hairpin
 281 N-terminal domain and the Fe, Mn SOD C-terminal domain (alpha-beta(2)-
 282 alpha-beta-alpha(2)). Values are consistent with the Mn-Sod from *Thermus*
 283 *thermophilus* [26], the closest homologue to *Borrelia* SodA with 51%
 284 sequence identity over 200 residues.

285

	α -helix	β -strand	β -turn	unordered
Apo-SodA	58 %	13 %	13 %	17 %
Fe-SodA	62 %	14 %	9 %	15 %
Mn-SodA	59 %	15 %	9 %	17 %

286

287 **Table 2.** Deconvolution of CD data for Apo-SodA, Fe-SodA and Mn-SodA.
 288 Proportion (%) of secondary structure types α -helix, β -strand, β -turn or
 289 unordered was determined using the CDSSTR method by DichroWeb [18, 27]
 290 using the SP175 dataset [28].

291

292 3.4 Mn activates *Borrelia* SodA and enhances protein folding

293

294 SOD activity was determined using an indirect colorimetric assay. Superoxide
 295 anions, produced by the oxidation of xanthine by xanthine oxidase, catalyze
 296 the reduction of WST-1 (2-(4-Iodophenyl)- 3-(4-nitrophenyl)-5-(2,4-
 297 disulfophenyl)-2H tetrazolium monosodium salt) to produce a formazan dye
 298 that absorbs light at 440 nm. SOD activity can be determined by measuring
 299 the inhibition of this reaction resulting from the removal of superoxide anions.

300

301 Apo-SodA and Fe-SodA failed to inhibit the enzyme activity colorimetric assay,
 302 giving average inhibition values close to zero (-1.1% \pm 5.2 and 1.5% \pm 6.3) and
 303 were not significantly different to each other ($P > 0.05$) (Fig. 3). This is in
 304 marked contrast to the Mn-SodA, which inhibited the reaction by 82.9% \pm 5.8.
 305 These data confirm that *Borrelia* SodA is Mn-dependent and not cambialistic.

306

307 The results demonstrate that *Borrelia* SodA was able to chelate Mn in the
 308 presence of 8 M urea, and that this Mn then remained bound to the enzyme
 309 during the subsequent refolding and purification steps resulting in active SodA.
 310 It is possible that some residual native structure exists that allows metal
 311 binding, even in the presence of 8 M urea. The refolding of apo-SodA was
 312 particularly problematic and gave a very low yield (0.9 mg/litre). Based on the
 313 improved yield of refolded protein in the presence of either Fe or Mn ions (8
 314 mg/l), it appears that metal binding improved protein-folding. These results

315 are in agreement with the literature. In live *Borrelia*, levels of SodA are
316 significantly reduced in a *bmtA* mutant unable to import Mn [15]. When
317 *Borrelia* SodA is heterogously expressed in the mitochondria or cytoplasm of
318 yeast cells, immunoblots revealed that protein is only detected when cells
319 were treated with 1 mM Mn [14]. This was demonstrated to be a stabilization
320 of polypeptide and not a transcriptional effect. Therefore, we propose that Mn-
321 binding by SodA promotes protein folding.
322

323 3.5 Homology model of dimeric Mn-SodA

324 The elution volume from size exclusion chromatography indicates that SodA
325 primarily exists as a homodimer (Fig. 1D). A homology model of the SodA
326 dimer was generated based on the tetrameric Mn-SOD from *T. thermophilus*
327 and the dimeric Mn-SOD from *E. coli* (Fig. 4). The primary sequence of
328 *Borrelia* SodA contains a single Cys residue (Cys136, Fig. 4). Because of the
329 reducing environment in the cytoplasm, most intracellular Cys residues would
330 not form a disulfide bond, however human SOD1 has been shown to contain
331 an intrasubunit disulfide [29], therefore the possible involvement of a disulfide
332 in the dimer interface in *Borrelia* SodA was important to consider. The
333 homology model of the SodA dimer revealed that the two Cys136 residues
334 are separated by ~43 Å and are therefore unlikely to be involved in an
335 intrasubunit disulfide without considerable rearrangement of the dimer
336 interface. This rearrangement is decidedly unlikely as residues at the dimer
337 interface are highly conserved between the *E. coli*, *T. thermophilus* and
338 *Borrelia* proteins with only a single amino acid difference observed,
339 Tyr34/Phe34 (Supplementary Table 1).

340 4 Conclusion

341 *Borrelia* SodA recombinantly expressed in *E. coli* can be refolded in the
342 presence of Mn. This therefore allows significant amounts of protein to be
343 produced for structural biology and biochemical studies. This Mn facilitates
344 protein folding and remains bound to the protein throughout the subsequent
345 purification steps. As demonstrated by indirect colorimetric assay, and
346 consistent with known literature, *Borrelia* SodA requires Mn for activity.
347 Finally, by studying a homology model of *Borrelia* SodA a single Cys residue
348 at the protein surface is revealed; this may stymie future attempts at
349 crystallography unless it is chemically blocked, effectively reduced or removed
350 by mutagenesis. .

351

352

353 *Conflict of interest*

354 *The authors declare no conflict of interest.*

355 *Author contributions*

356 GB, DCT, AHB, & SEC performed the research, analyzed the data and helped
357 to draft the manuscript;

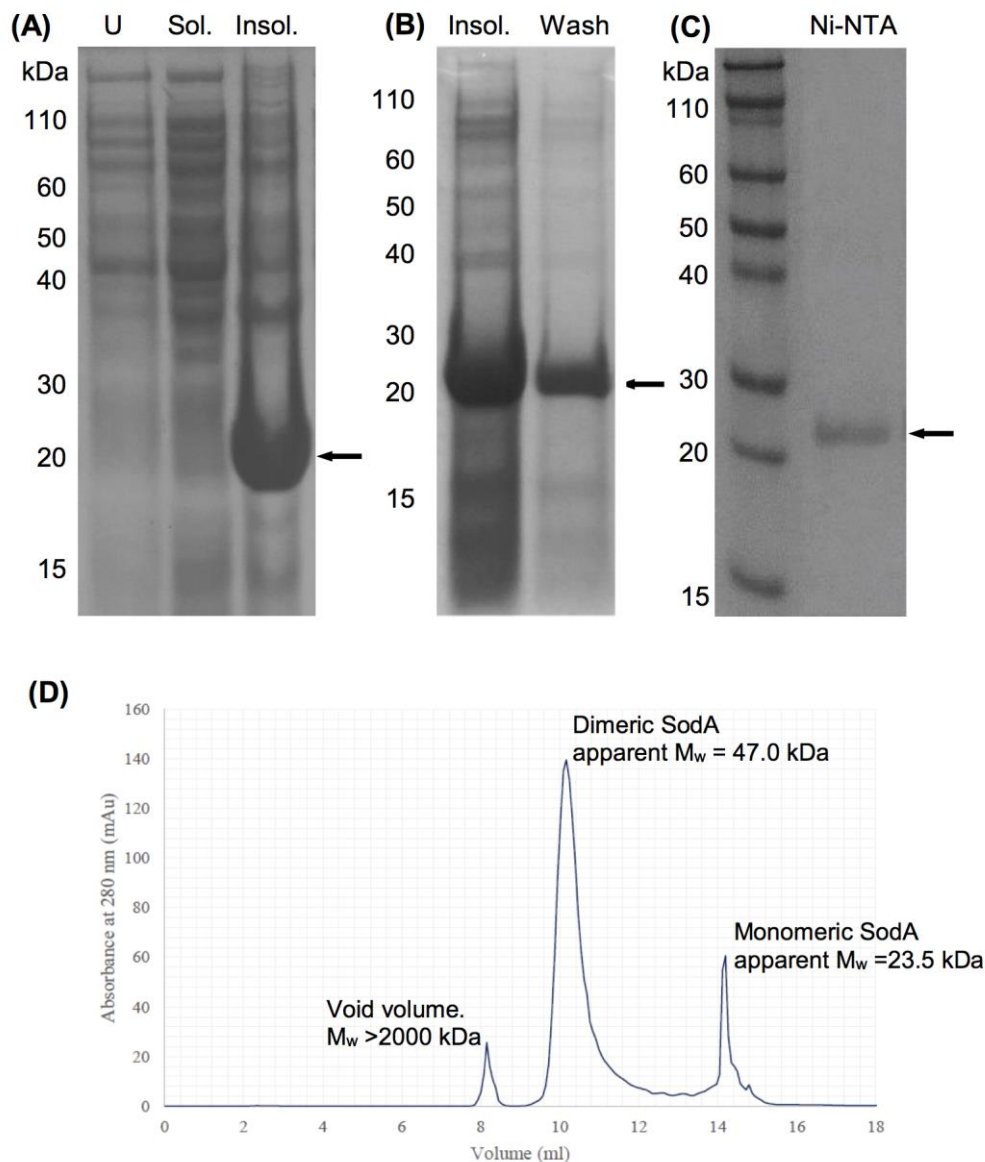
358 AD, AHB, GB, LS and RJB conceived and designed the work and wrote the
359 manuscript.

360 All authors contributed to and approved the final manuscript.

361

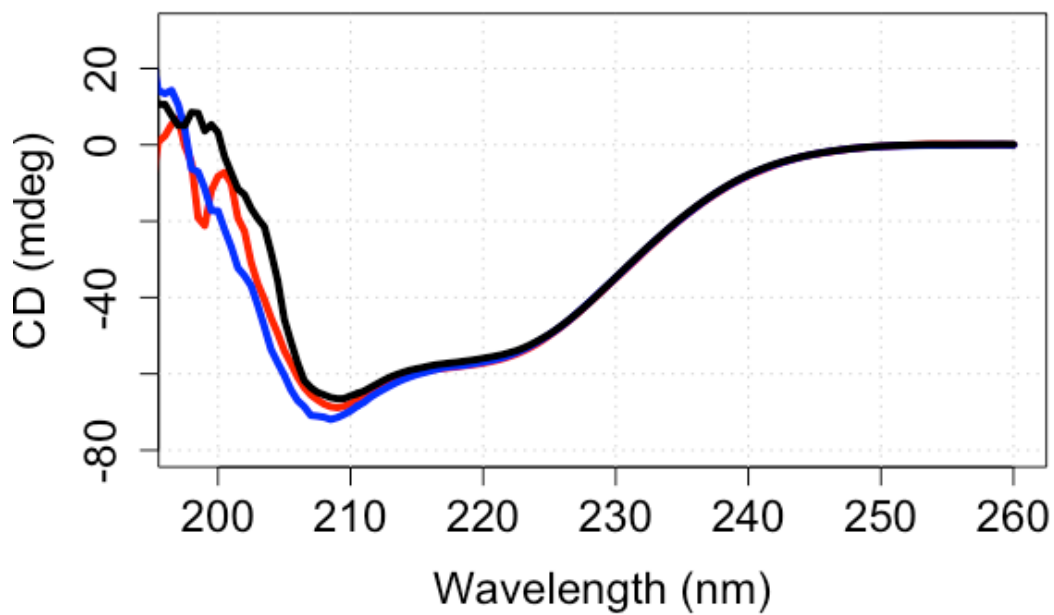
362 *Supplementary material*

363 **Supplementary Table 1** – Residues at the dimer interface of *E. coli*, *T.*
364 *thermophilus* and *B. burgdorferi* MnSODs



366

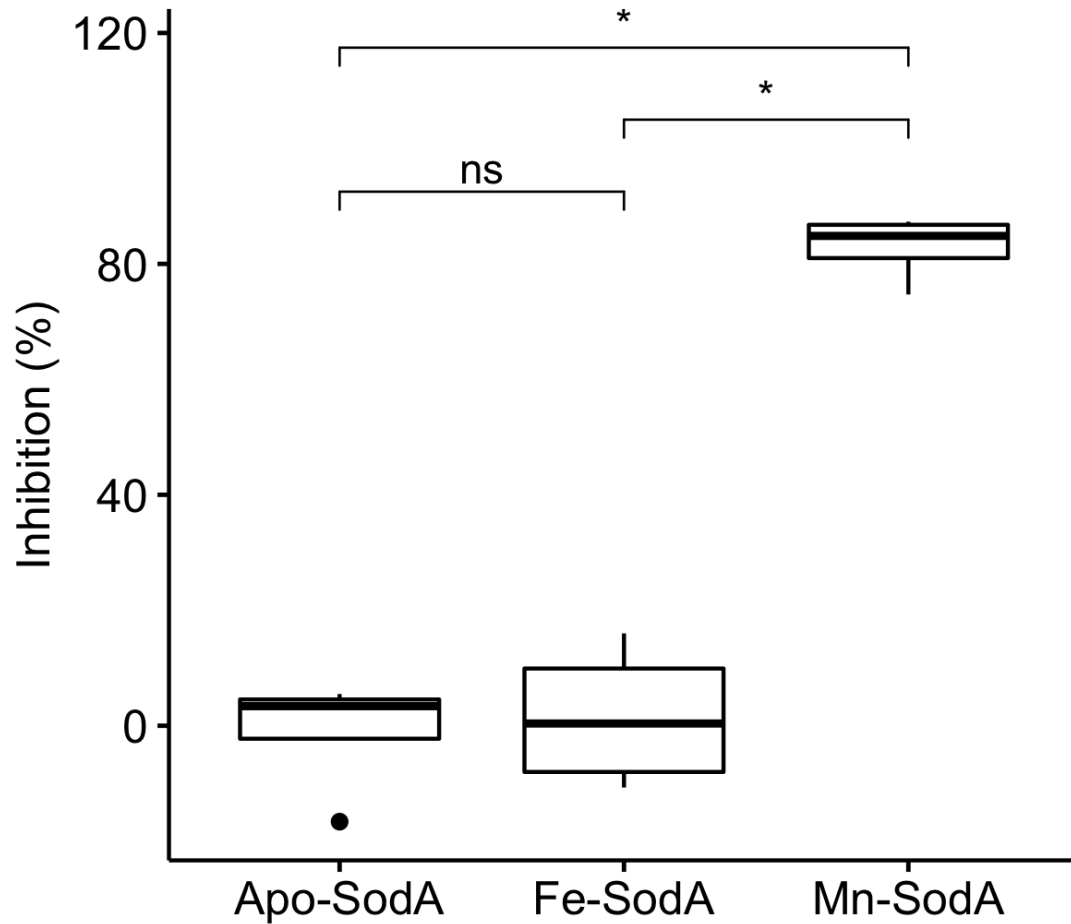
367 **Figure 1.** Purification and refolding of recombinant *Borrelia* SodA. (A) SDS-
 368 PAGE analysis of uninduced whole cell lysate (U), followed by post-induction
 369 soluble (Sol.) and insoluble (Insol.) cell lysate fractions. Recombinant *Borrelia*
 370 SodA is indicated by black arrows. (B) The insoluble pellet (Insol.) was
 371 washed six times as described in Methods (2.2) to generate a sample of
 372 inclusion bodies (Wash). (C) The inclusion bodies were then solubilized in 8 M
 373 urea and purified by immobilized metal affinity chromatography (Ni-NTA). (D)
 374 Size exclusion chromatography of *Borrelia* Mn-SodA. Fractions from both
 375 peaks were confirmed as SodA by enzyme assay.



376

377 **Figure 2.** Circular dichroism spectra of Apo-SodA (black), Fe-SodA (red) and
378 Mn-SodA (blue) at 20°C. Experiments were carried out on a Jasco J-810
379 spectropolarimeter. Experimental data was obtained over five individual scans
380 and averaged.

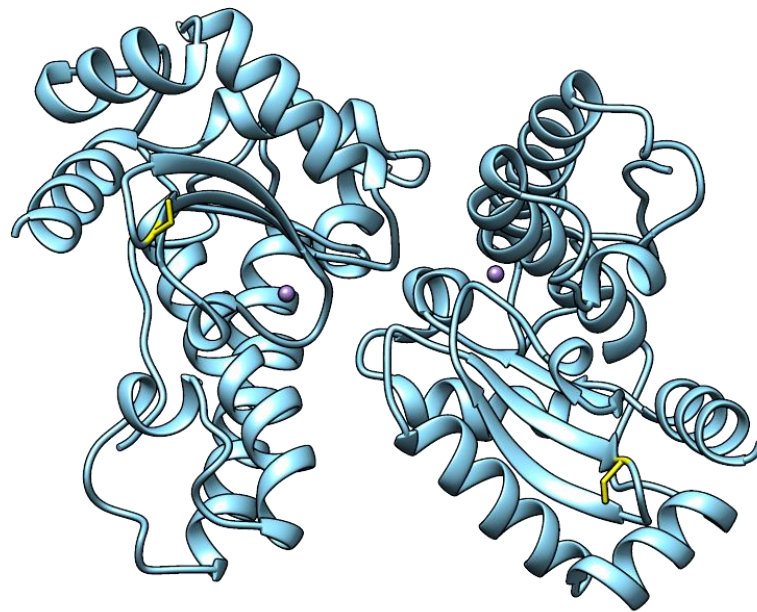
381



382

383 **Figure 3.** Activity of *B. burgdorferi* SodA refolded from 8M urea in the
 384 absence of metal ions (apo-SodA), or after addition of Fe/Mn. SOD activity
 385 was measured by an indirect enzyme assay based on the removal of
 386 superoxide anions from solution, preventing the reduction of WST-1 to
 387 formazan dye. Whiskers indicate the maximum and minimum of data, central
 388 bands indicate median values. Statistical analysis by ANOVA and a multiple
 389 comparison of sample means by Tukey's test revealed the enzyme activity of
 390 Mn-SodA to be significantly different to both Apo and Fe-SodA ($P < 0.05$).

391



392

393 **Figure 4.** Homology model of dimeric *Borrelia* SodA based on *T. thermophilus*
 394 and *E. coli* Mn-SODs generated using Phyre2. 203 residues were modelled at
 395 >90% accuracy. Mn shown as purple spheres. Cys136 shown using yellow
 396 sticks representation. The distance between the two Cys residues is ~43 Å.

397

398

399 References

- 400 [1] L. Benov, How superoxide radical damages the cell. *Protoplasma* 217
 401 (2001) 33-36.
- 402 [2] J.J. Perry, D.S. Shin, E.D. Getzoff, J.A. Tainer, The structural biochemistry of
 403 the superoxide dismutases. *Biochimica et biophysica acta* 1804 (2010) 245-262.
- 404 [3] M.W. Smith, R.F. Doolittle, A comparison of evolutionary rates of the two
 405 major kinds of superoxide dismutase. *J Mol Evol* 34 (1992) 175-184.
- 406 [4] P.E. Stewart, R. Byram, D. Grimm, K. Tilly, P.A. Rosa, The plasmids of
 407 *Borrelia burgdorferi*: essential genetic elements of a pathogen. *Plasmid* 53
 408 (2005) 1-13.
- 409 [5] C.M. Fraser, S. Casjens, W.M. Huang, G.G. Sutton, R. Clayton, R. Lathigra, O.
 410 White, K.A. Ketchum, R. Dodson, E.K. Hickey, M. Gwinn, B. Dougherty, J.F. Tomb,
 411 R.D. Fleischmann, D. Richardson, J. Peterson, A.R. Kerlavage, J. Quackenbush, S.
 412 Salzberg, M. Hanson, R. van Vugt, N. Palmer, M.D. Adams, J. Gocayne, J. Weidman,
 413 T. Utterback, L. Wathley, L. McDonald, P. Artiach, C. Bowman, S. Garland, C. Fuji,
 414 M.D. Cotton, K. Horst, K. Roberts, B. Hatch, H.O. Smith, J.C. Venter, Genomic
 415 sequence of a Lyme disease spirochaete, *Borrelia burgdorferi*. *Nature* 390 (1997)
 416 580-586.

417 [6] J.A. Boylan, K.A. Lawrence, J.S. Downey, F.C. Gherardini, *Borrelia*
418 burgdorferi membranes are the primary targets of reactive oxygen species. Mol
419 Microbiol 68 (2008) 786-799.

420 [7] J.E. Posey, F.C. Gherardini, Lack of a role for iron in the Lyme disease
421 pathogen. Science 288 (2000) 1651-1653.

422 [8] Z. Ouyang, M. He, T. Oman, X.F. Yang, M.V. Norgard, A manganese
423 transporter, BB0219 (BmtA), is required for virulence by the Lyme disease
424 spirochete, *Borrelia burgdorferi*. Proc Natl Acad Sci U S A 106 (2009) 3449-3454.

425 [9] P. Wang, A. Lutton, J. Olesik, H. Vali, X. Li, A novel iron- and copper-binding
426 protein in the Lyme disease spirochaete. Mol Microbiol 86 (2012) 1441-1451.

427 [10] T.A. Jackson, C.T. Gutman, J. Maliekal, A.F. Miller, T.C. Brunold, Geometric
428 and electronic structures of manganese-substituted iron superoxide dismutase.
429 Inorg Chem 52 (2013) 3356-3367.

430 [11] R. Wintjens, D. Gilis, M. Rooman, Mn/Fe superoxide dismutase interaction
431 fingerprints and prediction of oligomerization and metal cofactor from sequence.
432 Proteins 70 (2008) 1564-1577.

433 [12] M.D. Esteve-Gassent, N.L. Elliott, J. Seshu, sodA is essential for virulence of
434 *Borrelia burgdorferi* in the murine model of Lyme disease. Mol Microbiol 71
435 (2009) 594-612.

436 [13] C.A. Whitehouse, L.R. Williams, F.E. Austin, Identification of superoxide
437 dismutase activity in *Borrelia burgdorferi*. Infect Immun 65 (1997) 4865-4868.

438 [14] J.D. Aguirre, H.M. Clark, M. McIlvin, C. Vazquez, S.L. Palmere, D.J. Grab, J.
439 Seshu, P.J. Hart, M. Saito, V.C. Culotta, A manganese-rich environment supports
440 superoxide dismutase activity in a Lyme disease pathogen, *Borrelia burgdorferi*.
441 The Journal of biological chemistry 288 (2013) 8468-8478.

442 [15] B. Troxell, H. Xu, X.F. Yang, *Borrelia burgdorferi*, a pathogen that lacks iron,
443 encodes manganese-dependent superoxide dismutase essential for resistance to
444 streptonigrin. The Journal of biological chemistry 287 (2012) 19284-19293.

445 [16] M.M. Bradford, A rapid and sensitive method for the quantitation of
446 microgram quantities of protein utilizing the principle of protein-dye binding.
447 Anal Biochem 72 (1976) 248-254.

448 [17] L. Whitmore, B.A. Wallace, DICHROWEB, an online server for protein
449 secondary structure analyses from circular dichroism spectroscopic data. Nucleic
450 Acids Res 32 (2004) W668-673.

451 [18] L. Whitmore, B.A. Wallace, Protein secondary structure analyses from
452 circular dichroism spectroscopy: methods and reference databases. Biopolymers
453 89 (2008) 392-400.

454 [19] R.C. Team", R: A language and environment for statistical computing. R
455 Foundation for Statistical Computing Vienna, Austria URL [http://wwwR-](http://www.R-project.org/)
456 [projectorg/](http://www.R-project.org/) (2015).

457 [20] L.A. Kelley, S. Mezulis, C.M. Yates, M.N. Wass, M.J. Sternberg, The Phyre2
458 web portal for protein modeling, prediction and analysis. Nat Protoc 10 (2015)
459 845-858.

460 [21] E.F. Pettersen, T.D. Goddard, C.C. Huang, G.S. Couch, D.M. Greenblatt, E.C.
461 Meng, T.E. Ferrin, UCSF Chimera--a visualization system for exploratory research
462 and analysis. Journal of computational chemistry 25 (2004) 1605-1612.

463 [22] G. Chhetri, P. Kalita, T. Tripathi, An efficient protocol to enhance
464 recombinant protein expression using ethanol in *Escherichia coli*. MethodsX 2
465 (2015) 385-391.

- 466 [23] C.T. Privalle, W.F. Beyer, Jr., I. Fridovich, Anaerobic induction of ProMn-
467 superoxide dismutase in *Escherichia coli*. *The Journal of biological chemistry* 264
468 (1989) 2758-2763.
- 469 [24] E. Luk, M. Yang, L.T. Jensen, Y. Bourbonnais, V.C. Culotta, Manganese
470 activation of superoxide dismutase 2 in the mitochondria of *Saccharomyces*
471 *cerevisiae*. *The Journal of biological chemistry* 280 (2005) 22715-22720.
- 472 [25] R. Wintjens, C. Noel, A.C. May, D. Gerbod, F. Dufernez, M. Capron, E.
473 Viscogliosi, M. Rooman, Specificity and phenetic relationships of iron- and
474 manganese-containing superoxide dismutases on the basis of structure and
475 sequence comparisons. *The Journal of biological chemistry* 279 (2004) 9248-
476 9254.
- 477 [26] S. Sato, K. Nakazawa, Purification and properties of superoxide dismutase
478 from *Thermus thermophilus* HB8. *J Biochem* 83 (1978) 1165-1171.
- 479 [27] N. Sreerama, R.W. Woody, Estimation of protein secondary structure from
480 circular dichroism spectra: comparison of CONTIN, SELCON, and CDSSTR
481 methods with an expanded reference set. *Anal Biochem* 287 (2000) 252-260.
- 482 [28] J.G. Lees, A.J. Miles, F. Wien, B.A. Wallace, A reference database for circular
483 dichroism spectroscopy covering fold and secondary structure space.
484 *Bioinformatics* 22 (2006) 1955-1962.
- 485 [29] K. Sea, S.H. Sohn, A. Durazo, Y. Sheng, B.F. Shaw, X. Cao, A.B. Taylor, L.J.
486 Whitson, S.P. Holloway, P.J. Hart, D.E. Cabelli, E.B. Gralla, J.S. Valentine, Insights
487 into the role of the unusual disulfide bond in copper-zinc superoxide dismutase.
488 *The Journal of biological chemistry* 290 (2015) 2405-2418.
- 489